PLOS | ONE

RESEARCH ARTICLE

Bifurcation in Cell Cycle Dynamics Regulated by *p*53

Md. Jahoor Alam[1,2], Sanjay Kumar[3], Vikram Singh[4], R. K. Brojen Singh*[1]

1 School of Computational and Integrative Sciences, Jawaharlal Nehru University, New Delhi-110067, India, **2** College of Applied Medical Sciences, University of Hail, Hail-2440, Kingdom of Saudi Arabia, **3** Department of Computer Science, Jamia Millia Islamia, New Delhi 110025, India, **4** School of Life Sciences, Central University of Himachal Pradesh, Dharamshala-176215, India

* brojen@jnu.ac.in

Abstract

We study the regulating mechanism of *p*53 on the properties of cell cycle dynamics in the light of the proposed model of interacting *p*53 and cell cycle networks via *p*53. Irradiation (*IR*) introduce to *p*53 compel *p*53 dynamics to suffer different phases, namely oscillating and oscillation death (stabilized) phases. The *IR* induced *p*53 dynamics undergo collapse of oscillation with collapse time Δt which depends on *IR* strength. The stress *p*53 via *IR* drive cell cycle molecular species *MPF* and cyclin dynamics to different states, namely, oscillation death, oscillations of periods, chaotic and sustain oscillation in their bifurcation diagram. We predict that there could be a critical Δt_c induced by *p*53 via IR_c, where, if $\Delta t \langle \Delta t_c$ the cell cycle may come back to normal state, otherwise it will go to cell cycle arrest (apoptosis).

Citation: Alam MJ, Kumar S, Singh V, Singh RKB (2015) Bifurcation in Cell Cycle Dynamics Regulated by *p*53. PLoS ONE 10(6): e0129620. doi:10.1371/journal.pone.0129620

Academic Editor: Peiwen Fei, University of Hawaii Cancer Center, UNITED STATES

Received: November 22, 2014

Accepted: May 11, 2015

Published: June 19, 2015

Data Availability Statement: All relevant data are within the paper.

Funding: This work is financially supported by Department of Science and Technology (DST), New Delhi, India under sanction no. SB/S2/HEP-034/2012.

Competing Interests: The authors have declared that no competing interests exist.

Introduction

*p*53 is well known for its abnormally long stability in response to the stress available against genomic integrity [1]. It conglomerated with its negative inhibitor *MDM*2 in the nucleus due to their strong interaction [2]. When the cell is in stress condition (due to irradiation, stress inducer molecule etc), *p*53 concentration level rises which leads to cell cycle arrest until repair or doctoring takes place of the impaired DNA. If the repair is not successful the system goes towards the apoptosis [3–6]. The transcriptional ability of the *p*53 is kept under controlled level at normal state due to its negative feedback interaction with *MDM*2 [7]. The hyperbolized concentration of *MDM*2 helps in degradation of the *p*53 protein because of its E3-ligase activity, causing adherence of ubiquitin to the lysine rich C-terminal of the *p*53 molecule [8–10]. Introduction of stress in the system is sensed by the activation of *ARF* protein, initially situated in nucleolar region in the form of nucleophosmin shifts to the nucleoplasm in its independent and active cast, to mark *MDM*2 for its degradation, thus assisting the *p*53 stability [11–13]. Triggering of *p*53 in response to stress leads to the expression of several downstream genes apart from the *MDM*2.

*p*21 protein is one of the most important proteins which is found to be expressed due to *p*53 accumulation in the cell [14]. *p*53 acts as a transcription factor for *p*21. It is also reported that *p*21 expression is directly proportional to the level of *p*53 in the system [15]. The role of *p*21 in

controlling G1 phase checkpoint has been widely studied but its role in controlling G2 phase checkpoint is comparatively less studied [16–18]. The G2 phase checkpoint interruption leads to the disruption of cell cycle that leads to halt mitosis [14]. The cyclin-cdk interaction leads to the formation of *MPF* (Maturation Promoting Factor) [19]. The formation of *MPF* is very important for transition of G2 phase to mitosis phase [20]. The *p*21 protein is reported as antagonist for the formation of *MPF*. Several experimental results suggest that *p*21 directly interacts with *cdk* and also with cyclin leading to the inhibition of both *cdk* as well as cyclin [21]. It is also reported that the interaction of *cdk* and *p*21 causes to halt in DNA replication [20, 22].

Cyclin, in cell cycle process, is an important protein which interacts with cyclin dependent kinases and forms *MPF*. The *MPF* is responsible for the activation of pRb (Retinoblastoma protein), and helps the liberation of transcription factor *E2F* from its inhibitory. This *E2F* maintains the expression profile of genes required to ingress the S-phase of the cell division cycle [23–25]. Further, it is reported by several experimental results that *p*21 can directly interact with *MPF* and forms complex and then dissociate [16, 18]. Hence, *p*53 can able to cross talk with *MPF* and cyclin through *p*21.

There have been various experimental and theoretical studies on *p*53 regulatory network and cell cycle model to understand their regulatory mechanisms and cell fate. *p*53 – *Mdm*2 regulatory network has been modeled in order to study the impact of irradiation and change in DNA on cell variability and cell fate [26]. Further, it has also been shown that this DNA damage force the cell to select its fate (DNA repair, cell cycle arrest, apoptosis) via activating p53 [27]. On the other hand, variation in DNA methylation specially in neuronal cells in central nervous system may induce better response to developmental and environmental changes [28]. Moreover, this cell fate in tumor cells can probably be triggered by p53 dependent PUMA accumulation and p53 signal strength [29, 30]. Other method, say, recurrent artificial neural network model has also been implemented to study such network to understand DNA damage responses due to damage signal and parameter modeling to incorporate the changes [31, 32]. Studies in NF-kB model has been done in order to understand how the model system responses to the cellular signal which may trigger to different states like chaos in the dynamics and phase synchronization [33].

The experiments on mammalian cells show that p21-cyclin signaling pathway control the decision of cell cycle fate [34]. The other studies in cell cycle dynamics in mammalian cells further show the positive feedback as controlling mechanism of cell cycle regulation [35], role of noise in regulation and exhibition of bifurcation in cell cycle dynamics [36].

Our model incorporates the integration of both p53-Mdm2 regulatory network and cell cycle network in order to study the impact of p53 in deciding the fate of cell cycle dynamics and vice versa. We focus in this work to study and find out the behaviour of different molecular species which are actively involved in the checking of cell cycle at G2 phase regulated by *p*53. We proposed an integrated model of *p*53 and cell cycle network to find out the impact of *p*53 regulator on cell cycle via *p*21 protein. We organized our work as follows. We hope that the study may open up important behaviors in the dynamics of both *p*53 and cell cycle oscillators and in the decision making mechanism of cell fate via *p*53. We explained our proposed model in section II. The result of the large scale simulation of the model is given in section III with discussion. The conclusion based on our results is provided in section IV.

Materials and Methods

Model of cell cycle regulated by *p*53

We present a model which brings together *p*53 – *MDM*2 regulatory network [37] and cell cycle [38–40] via *p*21 protein (Fig 1) in the light of various theoretical and experimental reports. The

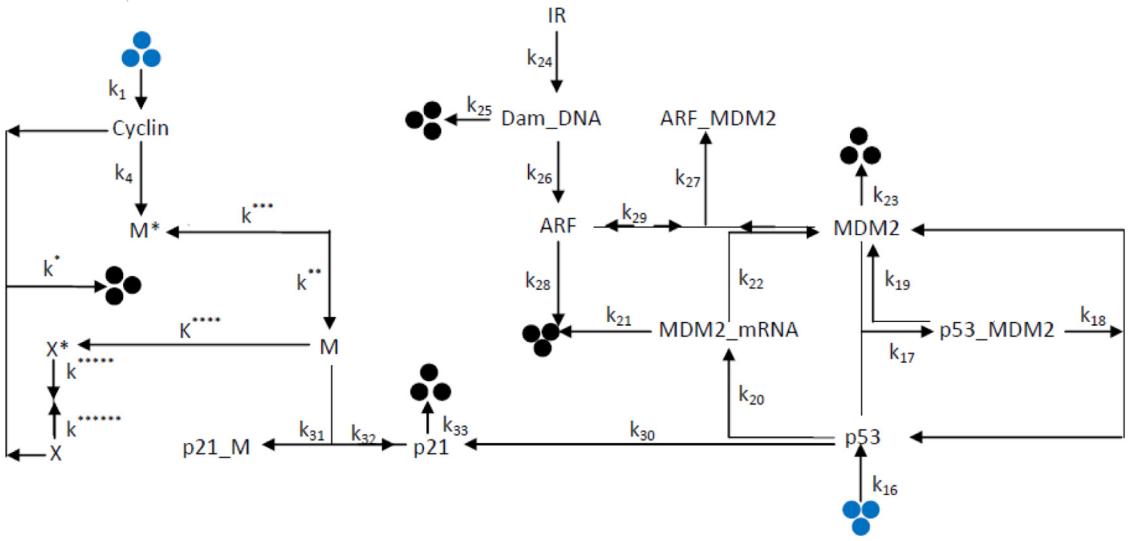

Fig 1. The schematic diagram of interaction of p53-Mdm2 reaction network cell cycle oscillator. The interaction between different molecular species are shown with respect to their rate constant. The blue and black dots indicate creation and decay of the respective molecular species.

doi:10.1371/journal.pone.0129620.g001

model is described briefly as follows. The main component of *p*53 – *MDM*2 regulatory network is the feedback loop between *p*53 and *MDM*2 [37]. *p*53 and *MDM*2 interact to form *p*53 – *MDM*2 complex with a rate constant k_{17} [37], followed by dissociation of the complex to its respective components with a rate constant k_{18} [41, 42]. The transcription rate of *MDM*2 gene to its *mRNA* (*MDM*2 – *mRNA*) is takes place with rate constant k_{20}, followed by translation of *MDM*2 – *mRNA* to *MDM*2 with a rate constant k_{22} [37, 43] and its (*MDM*2 – *mRNA*) self-degradation with a rate constant k_{21} [44]. The ubiqiutination of *MDM*2 protein occurs with rate constant k_{23}. The *p*53 synthesis is taken placed with a rate constant k_{16}, and gets ubiquitinized at the rate constant k_{19} [43]. The DNA damage in system is introduced via irradiation with an estimated rate constant of k_{24} [37]. Irradiation is reported to be a major cause of DNA damage. The severity of the DNA damage is depended on the dose of exposure of irradiation [34]. The repair of the DNA damage is then occurred at a rate constant k_{25} [45, 46]. The activation of *ARF* due to DNA damage takes place at a rate constant k_{26} [37]. Further, this activated form of *ARF* interacts with *MDM*2 protein and forms *ARF* – *MDM*2 complex with a rate constant k_{27} [47]. The degradation of *ARF* protein is reported to occur at a rate constant k_{28} [48]. *ARF* based degradation of the *MDM*2 takes place by getting targeted to the complex via proteasome recognition with a much faster rate constant k_{29} than individual degradation rates [49]. The *p*53, being a transcription promoting factor for many of the proteins, also transcribes the gene responsible for the manufacture of *p*21 protein with a rate constant k_{30} as presumed by the approximations made to attain the appropriate oscillations and arrests [14, 50, 51].

The *p*21 protein is capable of making complex with the cell division promoting factor *MPF* with a rate constant k_{31} [16, 18] with respect to the amount of concerned molecules present in the system [19]. Then the inhibition of *MPF*, or more appropriately G2 associated *Cyclin* – *Cdk* complex, by *p*21 is approximated with a rate constant k_{32} [50, 52]. *p*21 then gets degraded by the virtue of its half-life in the system with a rate constant k_{33} [18, 23]. The cyclin is assumed to translate at the rate constant k_1 [53]. Further, ubiquitin dependent cyclin degradation or protease independent degradation of the cyclin is reported to happen at a rate constant k^* [54]. The

degradation of the cyclin due to effect of protease activation during cyclin accumulation and interaction between inactive form of *MPF* with cyclin takes place with a rate constant k_4 [38]. Formation of activated form of *MPF* (M) occurs due to interaction of cyclin with inactive *MPF* (M^*) with a rate constant k^{**} [38, 55–57]. Further this activated form of *MPF* (M) converts to inactivated form (M^*)with a rate constant k^{***} [55, 57]. The activated form of *MPF*(M) interact with inactive protease(X^*) to generate activated form of protease (X) with a rate constant k^{****} [38, 58, 59]. The generation of activated form of cyclin protease (X) occurs due to interaction of cyclin protease with inactive X^* with a rate k^{*****} [38, 55]. The activated form of protease (X) can convert into inactive form (X^*) with a rate constant k^{******} [38, 57]. In Fig 1, The blue dots indicates creation and black dots indicates decay of the respective molecular species. The lists of molecular species and biochemical reaction channels involved in this proposed model are listed in Tables 1 and 2 respectively.

The biochemical reaction network shown in Fig 1 are represented by the twenty five reaction channels listed in Table 2, which are participated by thirteen molecular species (Table 1) defined by a vector at any instant of time t, $\mathbf{x}(t) = \{x_1(t), x_2(t), \ldots, x_N(t)\}^T$, where, T is the transpose of the vector and $N = 13$. The variables are the concentrations of the molecular species. The time evolution of these variables can be translated from the twenty five reaction channels into the following set of nonlinear ordinary differential equations (ODE) based on Mass action law of chemical kinetics,

$$
\begin{aligned}
\frac{dx_1}{dt} &= k_1 - \frac{k_2 x_1 x_3}{k_3 + x_1} - k_4 x_1 \\
\frac{dx_2}{dt} &= \frac{k_5(1 - x_2)}{x_6 + (1 - x_2)} - \frac{k_7 x_2}{k_8 x_2} - k_{31} x_{12} x_2 \\
\frac{dx_3}{dt} &= \frac{k_9(1 - x_3)}{k_{10} + (1 - x_3)} - \frac{k_{11} x_3}{k_{12} + x_3} \\
\frac{dx_4}{dt} &= k_{16} + k_{18} x_6 - k_{17} x_4 x_5 \\
\frac{dx_5}{dt} &= k_{22} x_7 + k_{19} x_6 + k_{18} x_6 - k_{23} x_5 - k_{17} x_5 x_4 \\
&\quad - k_{27} x_5 x_8 \\
\frac{dx_6}{dt} &= k_{17} x_4 x_5 - k_{18} x_6 - k_{19} x_6 \\
\frac{dx_7}{dt} &= k_{20} x_4 - k_{21} x_7 \\
\frac{dx_8}{dt} &= k_{26} x_{11} + k_{29} x_9 - k_{27} x_5 x_8 - k_{28} x_8 \\
\frac{dx_9}{dt} &= k_{27} x_5 x_8 - k_{29} x_9 \\
\frac{dx_{10}}{dt} &= -k_{24} x_{10} \\
\frac{dx_{11}}{dt} &= k_{24} x_{10} - k_{25} x_{11} \\
\frac{dx_{12}}{dt} &= k_{30} x_4 - k_{31} x_2 x_{12} + k_{32} x_{13} - k_{33} x_{12} \\
\frac{dx_{13}}{dt} &= k_{31} x_{12} x_2 - k_{32} x_{13}
\end{aligned}
$$

Table 1. List of molecular species.

S.No.	Species Name	Description	Notation
1.	*Cyclin*	Unbounded Cyclin protein	x_1
2.	*MPF*	Maturation promotion factor	x_2
3.	*Cyclin – Protease*	Unbounded Cyclin Protease	x_3
4.	*p*53	Unbounded *p*53 protein	x_4
5.	*Mdm*2	Unbounded *Mdm*2 protein	x_4
6.	*Mdm*2_*p*53	*Mdm*2 with *p*53 complex	x_6
7.	*Mdm*2_*mRNA*	*Mdm*2 messenger *mRNA*	x_7
8.	*ARF*	Unbounded *ARF* protein	x_8
9.	*ARF_Mdm*2	*ARF_Mdm*2 complex	x_9
10.	*IR*	Irradiation	x_{10}
11.	*DamDNA*	Damaged DNA	x_{11}
12.	*p*21	*p*21 protein	x_{12}
13.	*p*21_*M*	*p*21 and *M* complex	x_{13}

doi:10.1371/journal.pone.0129620.t001

where, the expressions for M^* and X^* in the Fig 1 are given by, $M^* = 1\text{-}x_{10}$ and $X^* = 1\text{-}x_{11}$. The set of coupled ODEs can be solved using Runge Kutta method of standard numerical integration algorithm [60].

Results and Discussion

We numerically simulate the proposed model and the results demonstrate new phenomena in bifurcation diagram which may be significant to correlate with various experimental situations. The interaction of *p*53 regulatory network and cell cycle network highlights different form of signal processing between non-identical networks which could be the way of regulating one another. We study the complicated way of this interaction in order to understand some of the basic mechanisms of network interaction.

Dynamics of *p*53 driven by irradiation

We first present the spatio-temporal behaviour of *p*53 upon exposure of irradiation in Fig 2. The *p*53 dynamics maintains minimum concentration level at $IR = 0$ (normal condition). As *IR* dose increases *p*53 start showing damped oscillatory behaviour (Fig 2 second and third panels) indicating stressed behaviour of *p*53. The increase in *IR* dose induces increase in time to attain stability of *p*53 dynamics (amplitude death) indicating increase in unstability of *p*53 dynamics (Fig 2 third panel). This could be due to the fact that the increase in *IR* dose may cause high DNA damage leading to more stress in *p*53.

However, if the *IR* dose is comparatively strong ($IR = 5$), the damage within the DNA is also high which may cause the collapse of the *p*53 oscillatory behaviour (Fig 2 fourth panel) and then repaired back the DNA damage to come back to *p*53 oscillatory condition. We also found that the time of collapse (Δt) increases as *IR* dose increases (Fig 2 fifth panel) and it becomes difficult to repair back the DNA damage. In general *p*53 will collapse forever and will not be recovered back if $\Delta t \rightarrow \infty$ (probable case of apoptosis). However, in real situation, one probably can define a critical Δt_c such that, if $\Delta t \langle \Delta t_c$, *p*53 could come back after DNA repair, and otherwise it will go to apoptosis. Nevertheless, it is very difficult to find out this Δt_c.

Similarly, we also present the plots of temporal variation of the concentration of *MDM*2 due to exposure of irradiation in right panels of Fig 2. We observed similar kind of behaviour as

Table 2. List of Chemical Reactions, Rate constants and their values.

S.No.	Biochemical reaction	Description	Rate Constant	Values of Rate Constant	Ref.
1	$\phi \xrightarrow{k_1} x_1$	Synthesis of Cyclin	k_1	$0.000416667 \times 10^{-2}\ sec^{-1}$	[38–40]
2	$x_1 \xrightarrow{k^*} \phi$	Decay of Cyclin	$k^*\langle x_1\rangle, where, k^* = \frac{k_2 x_1 x_3}{k_3 + x_1}$	$k_2 = 0.004166667 sec^{-1}$, $k_3 = 0.02 sec^{-1}$	[38, 54]
3	$x_1 \xrightarrow{k_4} \phi$	Cyclin decay	$k_4\langle x_1\rangle$	$0.0000167 sec^{-1}$	[38]
4	$\phi \xrightarrow{k^{**}} x_2$	Creation of MPF	$k^{**}, where, k^{**} = \frac{k_5(1-x_2)}{k_6+(1-x_2)}, k_5 = \frac{k_{14}x_1}{k_{13}+x_1}$	$k_6 = 0.01$, $k_{13} = 0.5$, $k_{14} = 0.00 sec^{-1}$	[16, 38, 57]
5	$x_2 \xrightarrow{k^{***}} \phi$	Decay of MPF	$k^{***}\langle x_2\rangle, where, k^{***} = \frac{k_7 x_2}{k_8 x_2}$	$k_7 = 0.0025 sec^{-1}$, $k_8 = 0.01 sec^{-1}$	[16, 55, 57]
6	$x_2 + x_{12} \xrightarrow{k_{31}} x_{13}$	Formation of *MPF_p21* complex	$k_{31}\langle x_2\rangle\langle x_{12}\rangle$	$0.0001 mol^{-1}\ sec^{-1}$	[16, 18, 19]
7	$\phi \xrightarrow{k_7} x_3$	Activation of protease molecule	$k^{****}, where, k^{****} = \frac{k_9(1-x_3)}{k_{10}+(1-x_3)}, k_9 = x_2 k_{15}$	$k_{10} = 0.01$, $k_{15} = 0.001667$	[38, 58, 59]
8	$x_3 \xrightarrow{k^{*****}} \phi$	Inactivation of protease molecule	$k^{*****}\langle x_3\rangle, where, k^{*****} = \frac{k_{11}x_3}{k_{12}+x_3}$	$k_{11} = 0.0008333$, $k_{12} = 0.01$	[38, 57]
9	$\phi \xrightarrow{k_{16}} x_4$	creation of p53	k_{16}	0.078	[37, 42, 43]
10	$x_4 + x_5 \xrightarrow{k_{17}} x_6$	synthesis of *p53_MDM2* complex	$k_{17}\langle x_4\rangle\langle x_5\rangle$	$1.155 \times 10^{-3}\ mol^{-1}\ sec^{-1}$	[37, 42]
11	$x_6 \xrightarrow{k_{18}} x_4 + x_5$	Dissociation of *p53_MDM2* complex	$k_{18}\langle x_6\rangle$	$1.155 \times 10^{-5}\ sec^{-1}$	[37, 41, 42]
12	$x_6 \xrightarrow{k_{19}} x_5$	ubiquitination of p53	$k_{19}\langle x_6\rangle$	$8.25 \times 10^{-4}\ sec^{-1}$	[37, 42, 43]
13	$x_4 \xrightarrow{k_{20}} x_4 + x_7$	creation of *MDM2_mRNA*	$k_{20}\langle x_4\rangle$	$1.0 \times 10^{-4}\ sec^{-1}$	[37, 42, 44]
14	$x_7 \xrightarrow{k_{21}} \phi$	decay of *MDM2_mRNA*	$k_{21}\langle x_7\rangle$	$1.0 \times 10^{-4}\ sec^{-1}$	[37, 42, 44]
15	$x_7 \xrightarrow{k_{22}} x_5 + x_7$	synthesis of MDM2	$k_{22}\langle x_7\rangle$	$4.95 \times 10^{-4}\ sec^{-1}$	[37, 42, 43]
15	$x_5 \xrightarrow{k_{23}} \phi$	decay of MDM2	$k_{23}\langle x_5\rangle$	$4.33 \times 10^{-4}\ sec^{-1}$	[37, 42, 43]
16	$x_{10} \xrightarrow{k_{24}} x_{11}$	creation of DNA damage	$k_{24}\langle x_{10}\rangle$	$1.0 sec^{-1}$	[37, 45]
17	$x_{11} \xrightarrow{k_{25}} \phi$	recovery of damaged DNA	$k_{25}\langle x_{11}\rangle$	$2.0 \times 10^{-5}\ sec^{-1}$	[37, 46]
18	$x_{11} \xrightarrow{k_{26}} x_8$	Activation of ARF	$k_{26}\langle x_{11}\rangle$	$3.3 \times 10^{-5}\ sec^{-1}$	[37]
19	$x_5 + x_8 \xrightarrow{k_{27}} x_9$	synthesis of *MDM2_ARF* complex	$k_{27}\langle x_5\rangle\langle x_8\rangle$	$0.01 mol^{-1}\ sec^{-1}$	[37, 47]
20	$x_8 \xrightarrow{k_{28}} \phi$	decay of ARF	$k_{28}\langle x_9\rangle\langle x_8\rangle$	$0.001 sec^{-1}$	[37, 48]
21	$x_9 \xrightarrow{k_{29}} x_8$	degradation of MDM2	$k_{29}\langle x_9\rangle$	$0.001 sec^{-1}$	[37, 49]
22	$x_4 \xrightarrow{k_{30}} x_4 + x_{12}$	synthesis of p21	$k_{30}\langle x_4\rangle$	$0.001 sec^{-1}$	[14, 50, 51]
23	$x_2 + x_{12} \xrightarrow{k_{30}} x_{13}$	synthesis of *p21_MPF* complex	$k_{31}\langle x_4\rangle$	$0.0001 sec^{-1}$	[14, 50, 51]
24	$x_{13} \xrightarrow{k_{32}} x_{12}$	dissociation of *p21_MPF* complex	$k_{32}\langle x_{13}\rangle$	$0.002 sec^{-1}$	[16, 18, 50]
25	$x_{12} \xrightarrow{k_{33}} \phi$	decay of p21 complex	$k_{33}\langle x_{12}\rangle$	$0.005 sec^{-1}$	[16, 50]

doi:10.1371/journal.pone.0129620.t002

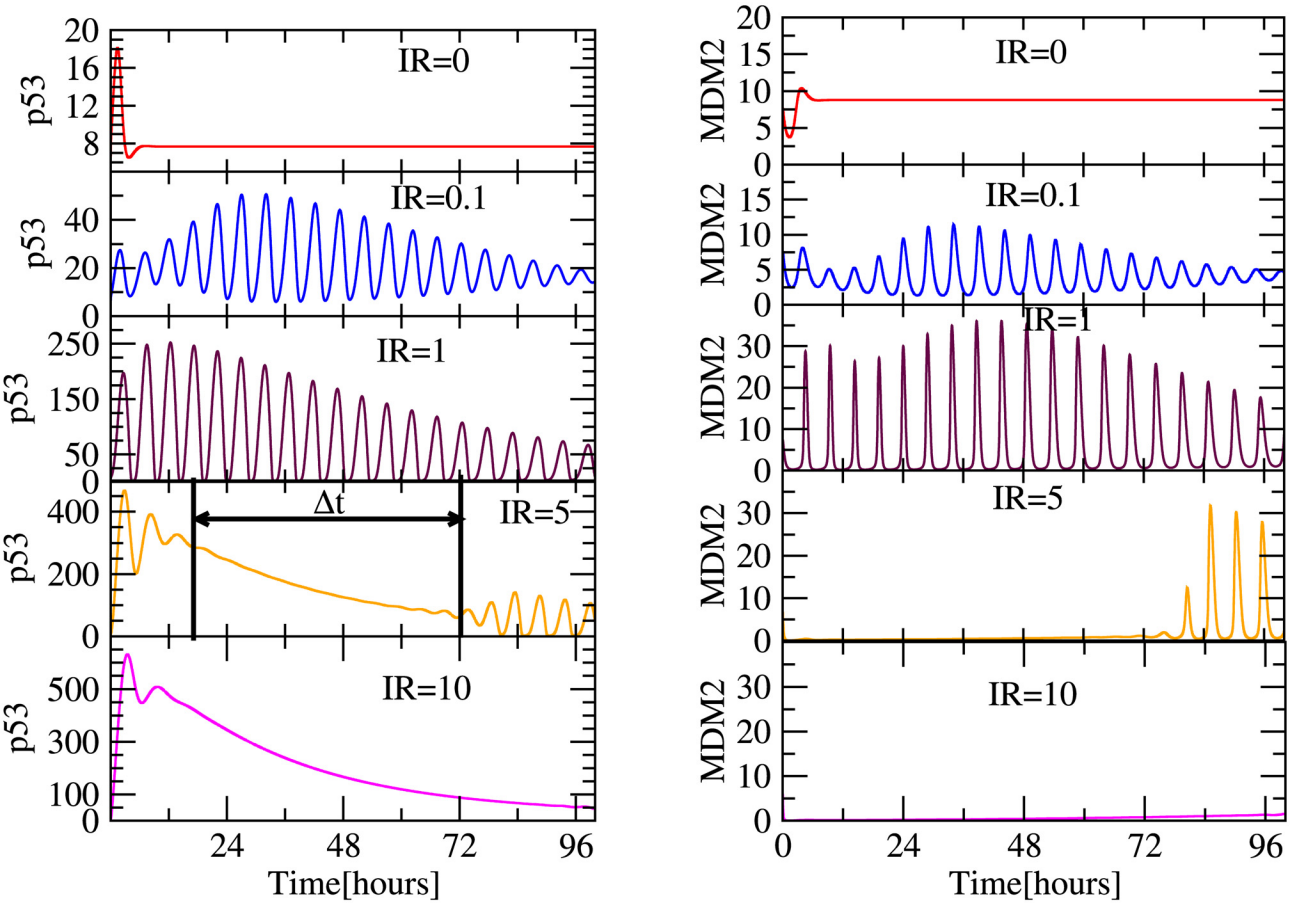

Fig 2. Plot shows the temporal variation in the concentration and oscillatory pattern of *p*53 protein due to the effect of various exposure of IR (Gy) i.e (0,0.1,1,5,10) in left panels. Similarly, temporal variation in the concentration and oscillatory pattern of *MDM2* protein due to the effect of various exposure of IR (Gy) i.e (0,0.1,1,5,10) are shown in right panels.

doi:10.1371/journal.pone.0129620.g002

obtained in case of *p*53 protein dynamics. This is probably due to intercorrelation between *p*53 and *MDM2* in the system via feedback mechanism. It is also noted that corresponding variations in the behaviours of both *p*53 and *MDM2* (as observed by comparing panels in Fig 2) are due to their positive as well as negative feedback regulations prescribed to them.

Phase diagram of *p*53 compelled by *IR*

We simulate the maxima of *p*53 amplitudes after removing the transients as a function of *IR* (Fig 3) to capture the different phases namely oscillation and oscillation death regimes. The behaviour of Δt as a function of *IR* follows the functional form $\Delta t = \frac{A}{B+e^{-IR}}$ with the values of $A = 6778$ and $B = 0.00887$ (fitting values of the function to the data) (Fig 3 inset). The separation between two phases oscillation death and oscillating regimes are clearly visible after the $IR \sim 3.45$ and Δt increases as *IR* increases.

Generally as $\Delta t \to \infty$ when $IR \to \infty$, but numerically we approximately found that after $IR = R_c \sim 11$ Δt become $\Delta t_c \sim 79$ hours and becomes constant (Fig 3 inset). This means that for any $\Delta t \langle \Delta t_c$, the *p*53 can able to recover back to normal stable state by repairing DNA damage, otherwise, the system can't able to come back to normal state, but will go to apoptosis.

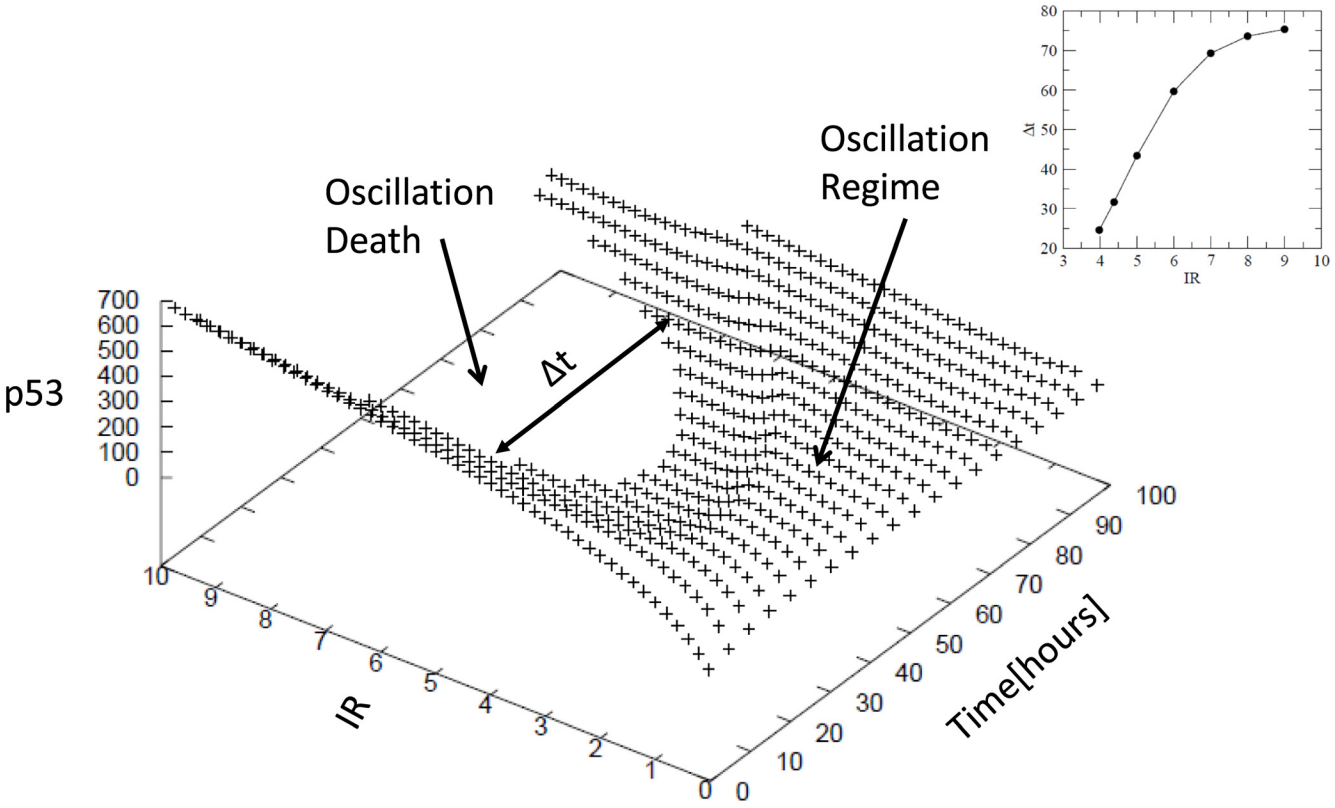

Fig 3. Plot for showing the impact of IR on p53 maxima. Different p53 maxima observed at different values of IR (Gy) with respect to time. The p53 maxima verses IR dose is shown at left hand side inset and also IR dose verses time is shown in right hand inset.

doi:10.1371/journal.pone.0129620.g003

Bifurcation in Cyclin regulated by *p*53

Since cell cycle and *p*53 regulatory networks are interacted through *p*21 (Fig 1), the temporal behaviour of cyclin can be regulated by *p*53 via *IR* and *p*21. When $IR = 0$, the two networks work in normal condition, leaving *p*53 dynamics at low level (stabilized state) (Fig 2 upper panel) and sustain oscillation in cyclin dynamics (Fig 4 upper left panel). As *IR* increases, *p*53 will get activated through DNA damage giving oscillatory behaviour affecting the dynamics of cyclin. When $IR = 0.1$, the cyclin dynamics shows chaotic behaviour upto $t = 145$ hours, and then the dynamics becomes sustain oscillation (Fig 4 second left panel and upper right panel). The chaotic behaviour in cyclin dynamics could due to the sudden activation in *p*53 dynamics due to *IR* irradiation.

Now as *IR* increases ($IR = 0.5$), we get various situations in the cyclin dynamics, namely, the emergence of period two (for $t \sim$ [10–40] hours), period 3 (for $t \sim$ [40–85] hours), chaotic regime (for $t \sim$ [85–175] hours) and sustain oscillation regime (for $t\rangle 175$ hours) (Fig 4 second right upper panel). Further, as *IR* increases the emergence of oscillation death regime started to exist in the cyclin dynamics (Fig 4 fourth right panel onwards) and the oscillation death regime become larger. Further increase in *IR* compels the period 2 and 3 regimes to vanish after some value of *IR* ($IR\rangle 9$) and the chaotic regime becomes larger.

The perturbation induced by *p*53 through *IR* to the cyclin via *p*21 clearly induces cyclin dynamics to various states shown by the bifurcation diagram (Fig 4 right panels). We also notice that as one decrease or increase to cross over to sustain oscillation, the state just before it is

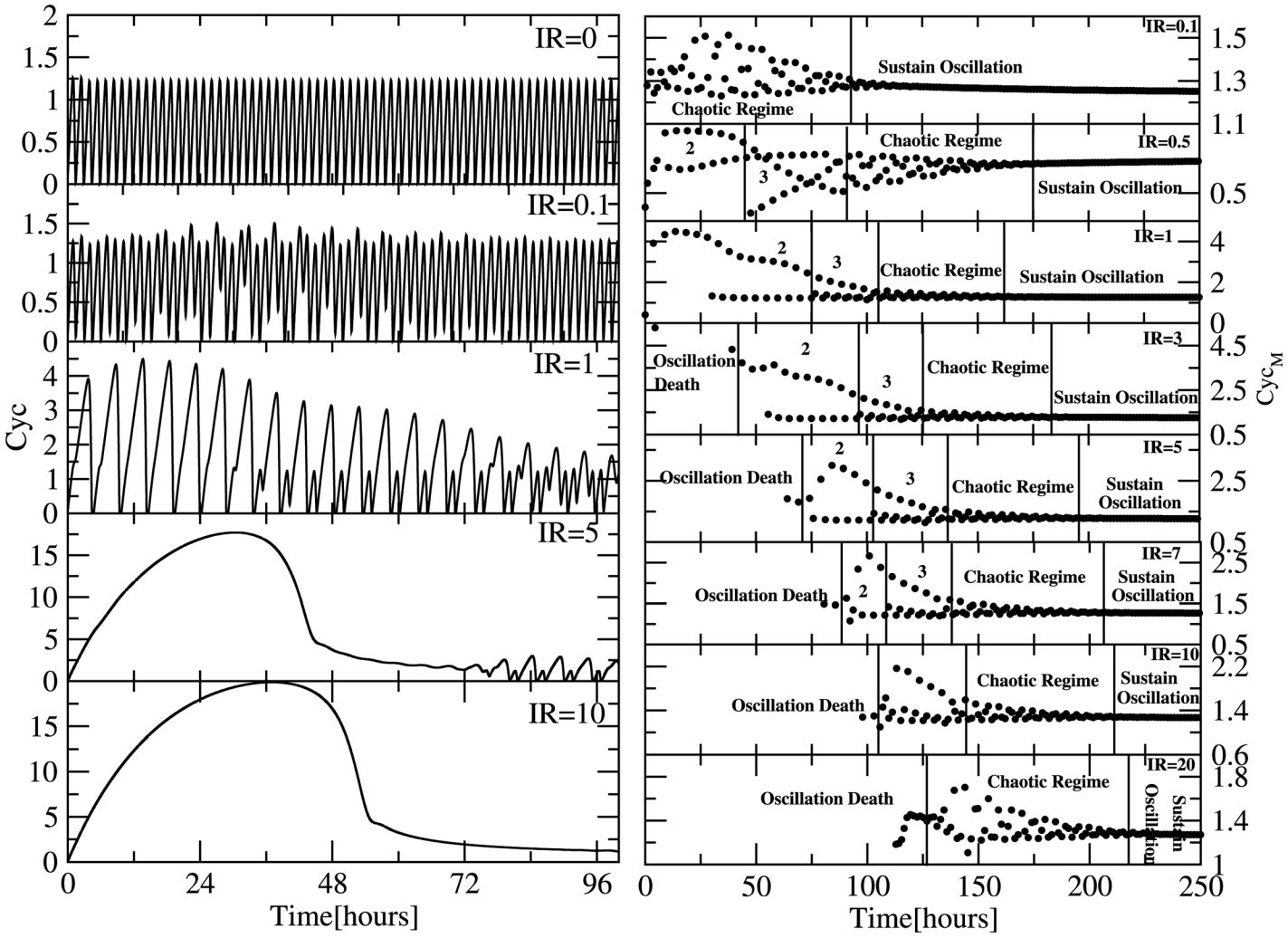

Fig 4. Plot shows the temporal variation in the oscillatory pattern of cyclin due to the effect of various exposure of IR (Gy) i.e (0,0.1,1,5,10) at left side panels and their corresponding bifurcation diagram are shown at right panels.

doi:10.1371/journal.pone.0129620.g004

chaotic regime. The emergence of oscillation death regime starts from $IR\rangle 3$ and then switches to sustain oscillation after sometime. This oscillation death regime corresponds to the collapse time due to strong sudden DNA damage. Once the DNA damage is recovered it comes back to sustain oscillation. If the *IR* is very large then oscillation death regime is large enough that DNA damage can not be repaired back halting the cell cycle permanantly and goes to apoptosis.

Dynamics of *MPF* regulated by *p*53

We present the temporal behaviour of *MPF* regulated by *p*53 as a function of *IR* (Fig 5) which induces at different states in *MPF* shown by bifurcation diagrams. The impact upon the *MPF* due to *p*53 via *IR* is not a direct phenomenon but through *p*21 molecule in the network. Various studies reported that *p*21 directly interact with cyclin dependent kinases, which has very important role in the formation of maturation promoting factor (MPF). The interaction of *p*21 with *cdk* leads to less availability of *cdk* due to the formation of *MPF*. Moreover, various

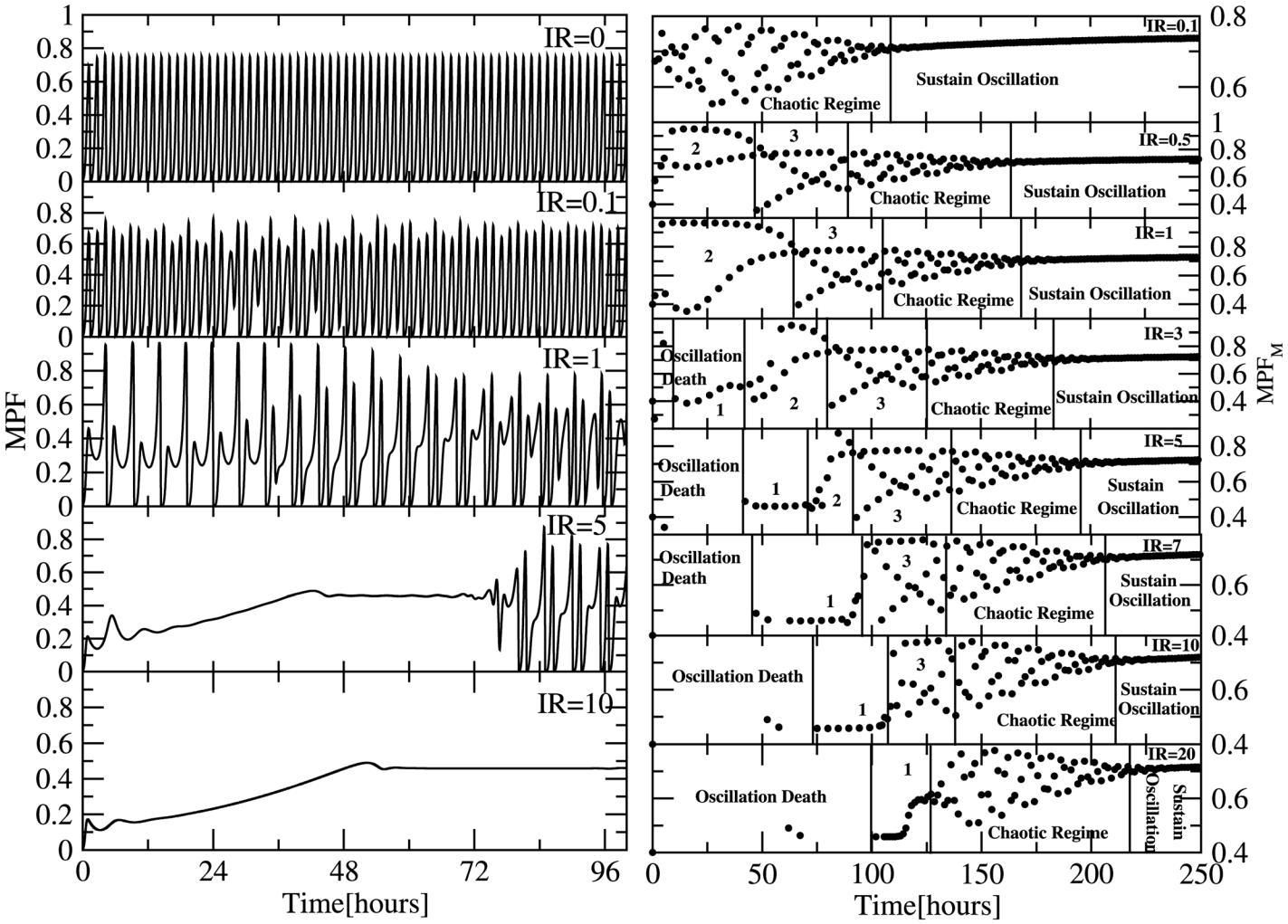

Fig 5. Plot shows the temporal variation in the oscillatory pattern of MPF(Maturation Promoting Factor) due to the effect of various exposure of IR (Gy) i.e (0,0.1,1,5,10) at left side panels and their corresponding bifurcation diagram are shown at right panels.

doi:10.1371/journal.pone.0129620.g005

experimental results also reported that *p*21 directly interacts with *MPF* [16, 18]. It is observed that an $IR = 0$, the *MPF* dynamics shows sustain oscillatory behaviour indicating no impact of *p*53. Further, as *IR* dose increases the oscillatory behaviour of *MPF* is abruptly changed inducing different states of *MPF* as we obtained in the case of cyclin. The increases in *IR* dose induce different states oscillation death, period 1, 2, 3, chaotic and sustain oscillation regimes indicated by the bifurcation diagram for various *IR* values. Moreover, as *IR* increases the width of oscillation death [16] regime also increases and if *IR* is not strong enough the DNA can able to repair back otherwise the system will go to apoptosis.

Bifurcation in *MPF* and Cyclin

We study the regulation of cell cycle dynamics by *p*53 via *IR*. The maxima values of *MPF* (MPF_M) and cyclin (Cyc_M) as a function of *IR* are calculated for a range of time in the range [0, 50] hours (Fig 6). It is observed that for low *IR* dose, MPF_M exhibits chaotic behaviour. However, if *IR* dose is comparatively high, MPF_M becomes almost constant. If the value of *IR* is

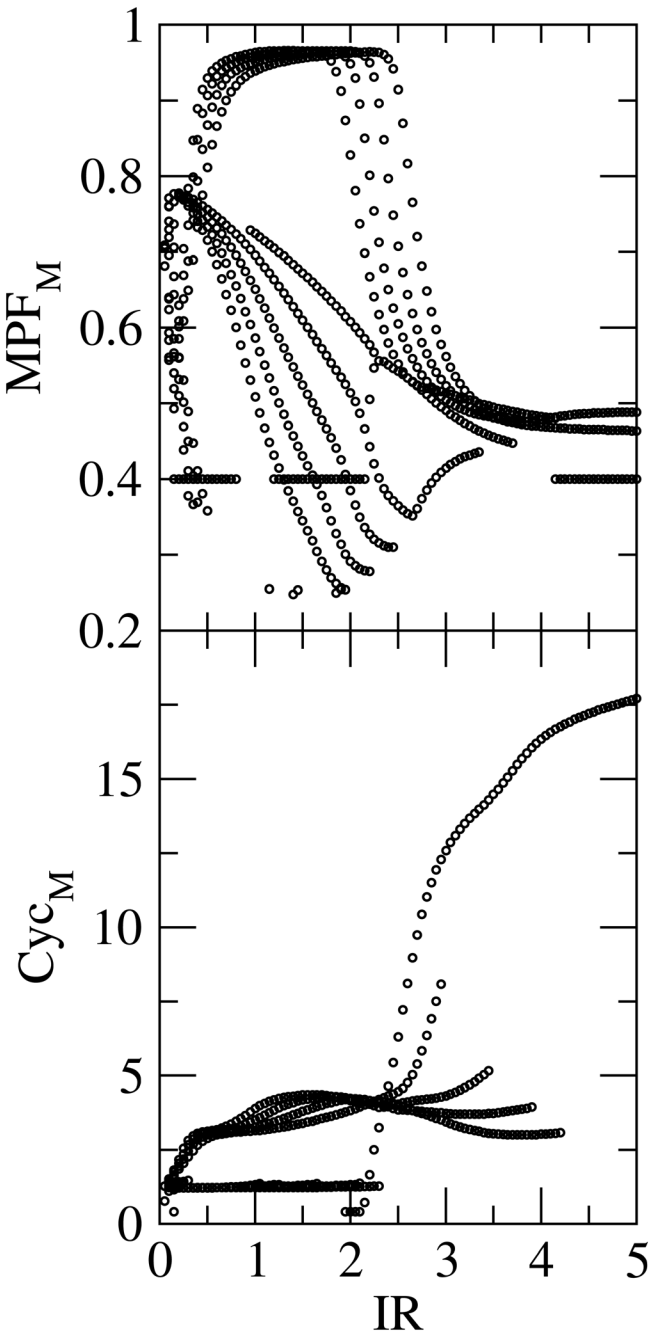

Fig 6. Plot shows the impact of various IR dose (in Gy) on MPF maxima (at upper panel) as well as Cyclin maxima (at lower panel).

doi:10.1371/journal.pone.0129620.g006

moderate, period 1, 2, 3 etc are exhibited in the bifurcation diagram. This indicates that MPF_M is *p*53 dependent via *IR* and *p*53 controls the MPF_M behaviour in the system.

Similarly, one can also observe the *IR* dependent maxima of cyclin Cyc_M in the bifurcation diagram (Fig 6 lower panel). The moderate values of *IR* induce different periods in Cyc_M. Excess values of *IR* show different behaviour in Cyc_M.

Conclusion

We study the way how *p*53, one of the largest hubs in cellular network, regulates and controls cell cycle dynamics. We studied the behaviour of different molecules which are highly involved in the checking of cell cycle at G2 phase driven by *p*53 via *IR*. The simulation results of the model provided us to understand the biological phenomenon and mechanism of cell cycle arrest due to DNA damage faced by the cell due to the irradiation. The results we got are closely in agreement with the previous experimental reports [16, 17]. Our study suggests that the temporal dynamics of molecular species involved in cell cycle, considered in the model, are controlled by *p*53. The role of *p*21 protein in the delay of G2 phase was considered as a cross-talk between *p*53 regulatory network and cell cycle. The sudden irradiation to the system with high dose induces collapse of the system due to DNA damage, leading to cell cycle arrest. The cell cycle is resumed again to normal situation by repairing back the DNA damage. Moreover, the time of recovery from cell cycle arrest and then resumption of oscillation depends on the amount of dose of *IR* exposed to the system.

During the process of regulation of cell cyle by *p*53 via *IR* we observed the emergence of different periods (1, 2, 3 etc) in the bifurcation diagram of oscillatory dynamics of cell cycle variables (MPF_M and Cyc_M) which may have various information of certain biological significance. Further, the dynamics of these variables switched to various states, namely, chaotic, oscillation death (stabilized state), bifurcating to various periods of oscillation and sustain oscillation states during the process of time evolution. These states could be the different phases of the variables to self-recover back to its normal condition from the sudden stress given to the system. However, how these complicated states are used by the system dynamics when the system is perturbed need to be investigated further.

The study also demonstrates the mechanism of cell cycle arrest induced by perturbed *p*53 via *IR* indicated by collapse of the oscillation (oscillation death) for certain interval of time (Δt). This collapse time is a function of strength of the perturbation imparted to the system. Our study shows that there is a minimum value of $IR = R_c$, below which the system comes back to its normal state, otherwise the system will go to apoptosis. Our findings will probably be useful for the further study on the impact of *p*53 on cell cycle checking at G2 phase and related dynamics.

Author Contributions

Conceived and designed the experiments: MJA RKBS. Performed the experiments: MJA SK RKBS. Analyzed the data: MJA VS RKBS. Contributed reagents/materials/analysis tools: MJA RKBS. Wrote the paper: MJA RKBS.

References

1. Lane DP (1992) p53, guardian of the genome. Nature 358:15–16. PMID: 1614522
2. Mendrysa SM, Perry ME (2000) The p53 tumor suppressor protein does not regulate expression of its own inhibitor, MDM2, except under conditions of stress. Mol. Cell. Biol. 20:2023–2030. doi: 10.1128/MCB.20.6.2023-2030.2000 PMID: 10688649
3. Michael D, Oren M (2002) The p53 and Mdm2 families in cancer. Curr. Opin. Genet. Dev. 12:53–59. doi: 10.1016/S0959-437X(01)00264-7 PMID: 11790555

4. Bargonetti J, Manfredi JJ (2002) Multiple roles of the tumor suppressor p53. Curr. Opin. Oncol. 14: 86–91. doi: 10.1097/00001622-200201000-00015 PMID: 11790986
5. Vogelstein B, Lane D, Levine AJ (2000) Surfing the p53 network Nature 408:307–310. doi: 10.1038/35042675 PMID: 11099028
6. Vousden KH (2000) p53: death star. Cell 103:691–694. doi: 10.1016/S0092-8674(00)00171-9 PMID: 11114324
7. Momand J, Wu HH, Dasgupta G (2000) MDM2–master regulator of the p53 tumor suppressor protein. Gene 242:15–29. doi: 10.1016/S0378-1119(99)00487-4 PMID: 10721693
8. Maki CG, Huibregtse JM, Howley PM (1996) In vivo ubiquitination and proteasome-mediated degradation of p53(1). Cancer Res. 56:2649–2654. PMID: 8653711
9. Honda R, Tanaka H, Yasuda H (1997) Oncoprotein MDM2 is a ubiquitin ligase E3 for tumor suppressor p53. FEBS Lett. 420:25–27. doi: 10.1016/S0014-5793(97)01480-4 PMID: 9450543
10. Scheffner M, Huibregtse JM, Vierstra RD, Howley PM (1993) The HPV-16 E6 and E6-AP complex functions as a ubiquitin-protein ligase in the ubiquitination of p53. Cell 75:495–505. doi: 10.1016/0092-8674(93)90384-3 PMID: 8221889
11. Pomerantz J, Schreiber-Agus N, Ligeois NJ, Silverman A, Alland L, Lynda C et al. (1998) The Ink4a tumor suppressor gene product, p19Arf, interacts with MDM2 and neutralizes MDM2's inhibition of p53. Cell 92:713–723. doi: 10.1016/S0092-8674(00)81400-2 PMID: 9529248
12. Honda R, Yasuda H (1999) Association of p19(ARF) with Mdm2 inhibits ubiquitin ligase activity of Mdm2 for tumor suppressor p53. EMBO J. 18:22–27. doi: 10.1093/emboj/18.1.22 PMID: 9878046
13. Midgley CA, Desterro JM, Saville MK, Howard S, Sparks A, Hay RT, et al. (2000) An N-terminal p14ARF peptide blocks Mdm2-dependent ubiquitination in vitro and can activate p53 in vivo. Oncogene 19:2312–2323. doi: 10.1038/sj.onc.1203593 PMID: 10822382
14. El-Deiry WS, Tokino T, Velculescu VE, Levy DB, Parsons R, Jeffrey M, et al. (1993) WAF1, a potential mediator of p53 tumor suppression. Cell 75:817–825. doi: 10.1016/0092-8674(93)90500-P PMID: 8242752
15. Gariel AL, Radhakrishnan SK (2005) Lost in transcription: p21 repression, mechanisms, and consequences. Cancer Res. 65:3980–3985. doi: 10.1158/0008-5472.CAN-04-3995
16. Bunz F, Dutriaux A, Lengauer C, Waldman T, Zhou S, Brown JM et al. (1998) Requirement for p53 and p21 to Sustain G2 Arrest After DNA Damage. Science 282:1497–1501. doi: 10.1126/science.282.5393.1497 PMID: 9822382
17. Bates S, Ryan KM, Phillips AC, Vousden KH (1998) Cell cycle arrest and DNA endoreduplication following p21Waf1/Cip1 expression. Oncogene 17:1691–1703. doi: 10.1038/sj.onc.1202104 PMID: 9796698
18. Aguda BD (1999) A quantitative analysis of the kinetics of the G(2) DNA damage checkpoint system. Proc. Natl. Acad. Sci. USA, 96:11352–11357. doi: 10.1073/pnas.96.20.11352 PMID: 10500180
19. Harper JW, Adami GR, Wei N, Keyomarsi K, Elledge SJ (1993) The p21 Cdk-interacting protein Cip1 is a potent inhibitor of G1 cyclin-dependent kinases. Cell 75:805–816. doi: 10.1016/0092-8674(93)90499-G PMID: 8242751
20. Aprelikova O, Xiong Y, Liu ET (1995) Both p16 and p21 families of cyclin-dependent kinase (CDK) inhibitors block the phosphorylation of cyclin-dependent kinases by the CDK-activating kinase. J. Biol. Chem. 270:18195–18197. doi: 10.1074/jbc.270.31.18195 PMID: 7629134
21. Funk JO, Waga S, Harry JB, Espling E, Stillman B and Galloway DA. (1997) Inhibition of CDK activity and PCNA-dependent DNA replication by p21 is blocked by interaction with the HPV-16 E7 oncoprotein. Genes Dev. 11:2090–2100. doi: 10.1101/gad.11.16.2090 PMID: 9284048
22. Soria G, Speroni J, Podhajcer OL, Prives C, Gottifredi V (2008) p21 differentially regulates DNA replication and DNA-repair-associated processes after UV irradiation. J. Cell Sci. 121:3271–3282. doi: 10.1242/jcs.027730 PMID: 18782865
23. Resnitzky D, Reed SI (1995) Different roles for cyclins D1 and E in regulation of the G1-to-S transition. Mol. Cell. Biol. 15:3463–3469. PMID: 7791752
24. Hinds PW, Weinberg RA (1994) Tumor suppressor genes. Curr. Opin. Genet. Dev. 4:135–141. doi: 10.1016/0959-437X(94)90102-3 PMID: 8193533
25. Lam EW, La Thangue NB (1994) DP and E2F proteins: coordinating transcription with cell cycle progression. Curr. Opin. Cell Biol. 6:859–866. doi: 10.1016/0955-0674(94)90057-4 PMID: 7880534
26. Iwamoto K, Hiroyuki H, Yukihiro E, Masahiro O (2014) Stochasticity of Intranuclear Biochemical Reaction Processes Controls the Final Decision of Cell Fate Associated with DNA Damage. PLOS One 9: e101333. doi: 10.1371/journal.pone.0101333 PMID: 25003668

27. Iwamotoa K, Hiroyuki H, Yukihiro E and Masahiro Okamoto (2011) Mathematical modeling of cell cycle regulation in response to DNA damage: Exploring mechanisms of cell-fate determination. Biosystems 103: 384–391. doi: 10.1016/j.biosystems.2010.11.011

28. Iwamoto K, Miki B, Junko U, Michael CO, Wataru U, Eri H, et al. (2015) Neurons show distinctive DNA methylation profile and higher interindividual variations compared with non-neurons. Cold Spring Harbor Laboratory Press 21:688–696.

29. Sun T, Chun C, Wu Y, Shuai Z, Jun C and Shen P. (2009) Modeling the role of p53 pulses in DNA damage- induced cell death decision. BMC Bioinf. 10:190. doi: 10.1186/1471-2105-10-190

30. Chonga KH, Sandhya S and Kulasiri D (2015) Mathematical modelling of p53 basal dynamics and DNA damage response. Math. Biosc. 259:2742.

31. Ling H, Sandhya S and Kulasiri D (2013) Ovel recurrent neural network for modelling biological networks: Oscillatory p53 interaction dynamics. Biosystems 114:191205. doi: 10.1016/j.biosystems.2013.08.004

32. Chen X, Chen J, Gan S, Guan H, Zhou Y, Qi O, et al. (2013) DNA damage strength modulates a bimodal switch of p53 dynamics for cell-fate control. BMC Biology 11:73. doi: 10.1186/1741-7007-11-73 PMID: 23800173

33. Jensen MH and Sandeep K (2012) Inducing phase-locking and chaos in cellular oscillators by modulating the driving stimuli. FEBS Lett. 586:16641668.

34. Chen J, Jia-Ren L, Tsai FC, Meyer T (2013) Dosage of Dyrk1a Shifts Cells within a p21-Cyclin D1 Signaling Map to Control the Decision to Enter the Cell Cycle. Mol. Cell 52: 87100. doi: 10.1016/j.molcel.2013.09.009

35. Grard C, Goldbeter H (2012) From quiescence to proliferation: Cdk oscillations drive the mam malian cell cycle. Front. Physiol. 3:413.

36. Ferrell Jr. JE, Pomerening JR, Sun YK, Nikki BT, Wen X, Frederick CY, et al. (2009) Simple, realistic models of complex biological processes: Positive feedback and bistability in a cell fate switch and a cell cycle oscillator. FEBS Lett. 583:39994005. doi: 10.1016/j.febslet.2009.10.068

37. Proctor CJ, Gray DA (2008) Explaining oscillations and variability in the p53-Mdm2 system. BMC Syst. Biol. 2:75. doi: 10.1186/1752-0509-2-75 PMID: 18706112

38. Goldbeter A (1991) A minimal cascade model for the mitotic oscillator involving cyclin and cdc2 kinase. Proc. Natl. Acad. Sci. U. S. A. 88:9107–9111. doi: 10.1073/pnas.88.20.9107 PMID: 1833774

39. Nurse P (1990) Universal control mechanism regulating onset of M-phase. Nature 344:503–508. doi: 10.1038/344503a0 PMID: 2138713

40. Murray AW, Kirschner MW (1989) Dominoes and clocks: the union of two views of the cell cycle. Science 246:614–621. doi: 10.1126/science.2683077 PMID: 2683077

41. Moll UM, Petrenko O (2003) The MDM2-p53 interaction. Mol. Cancer Res. 1:1001–1008. PMID: 14707283

42. Alam MJ, Devi GR, Ravins, Ishrat R, Agarwal SM and Singh RKB. (2013) Switching p53 states by calcium: dynamics and interaction of stress systems. Mol. BioSyst. 9:508–521. doi: 10.1039/c3mb25277a PMID: 23360948

43. Finlay CA (1993) The mdm-2 oncogene can overcome wild-type p53 suppression of transformed cell growth. Mol. Cell. Biol. 13:301–306. PMID: 8417333

44. Lahav G, Rosenfeld N, Sigal A, Geva-Zatorsky N, Levine AJ, Elowitz MB, et al. (2004) Dynamics of the p53-Mdm2 feedback loop in individual cells. Nat. Genet. 36:147–150. doi: 10.1038/ng1293 PMID: 14730303

45. Vilenchik MM, Knudson AG (2003) Endogenous DNA double-strand breaks: production, fidelity of repair, and induction of cancer. Proc. Natl. Acad. Sci. U. S. A. 100:12871–12876. doi: 10.1073/pnas.2135498100 PMID: 14566050

46. Schultz LB, Chehab NH, Malikzay A, Halazonetis TD (2000) p53 binding protein 1 (53BP1) is an early participant in the cellular response to DNA double-strand breaks. J. Cell Biol. 151:1381–1390. doi: 10.1083/jcb.151.7.1381 PMID: 11134068

47. Khan S, Guevara C, Fujii G, Parry D (2004) p14ARF is a component of the p53 response following ionizing irradiation of normal human fibroblasts. Oncogene 23:6040–6046. doi: 10.1038/sj.onc.1207824 PMID: 15195142

48. Kuo ML, den Besten W, Bertwistle D, Roussel MF, Sherr CJ (2004) N-terminal polyubiquitination and degradation of the Arf tumor suppressor. Genes Dev. 18:1862–1874. doi: 10.1101/gad.1213904 PMID: 15289458

49. Zhang Y, Xiong Y, Yarbrough WG (1998) ARF promotes MDM2 degradation and stabilizes p53: ARF-INK4a locus deletion impairs both the Rb and p53 tumor suppression pathways. Cell 92:725–734 doi: 10.1016/S0092-8674(00)81401-4 PMID: 9529249

50. Xiong Y, Hannon GJ, Zhang H, Casso D, Kobayashi R and David B. (1993) p21 is a universal inhibitor of cyclin kinases. Nature 366:701–704. doi: 10.1038/366701a0 PMID: 8259214

51. el-Deiry WS, Harper JW, Connor PM, Velculescu VE, Canman CE, Joany J, et al. (1994) WAF1/CIP1 is induced in p53-mediated G1 arrest and apoptosis. Cancer Res. 54:1169–1174. PMID: 8118801

52. Waga S, Hannon GJ, Beach D, Stillman B (1994) The p21 inhibitor of cyclin-dependent kinases controls DNA replication by interaction with PCNA. Nature 369:574–578. doi: 10.1038/369574a0 PMID: 7911228

53. Morla AO, Draetta G, Beach D, Wang JY (1989) Reversible tyrosine phosphorylation of cdc2: dephosphorylation accompanies activation during entry into mitosis. Cell 58:193–203. doi: 10.1016/0092-8674(89)90415-7 PMID: 2473839

54. Strausfeld U, Labbe JC, Fesquet D, Cavadore JC, Picard A, Sadhu K, et al. (1991) Dephosphorylation and activation of a p34cdc2/cyclin B complex in vitro by human CDC25 protein. Nature 351: 242–245. doi: 10.1038/351242a0 PMID: 1828290

55. Murray AW, Solomon MJ, Kirschner MW (1989) The role of cyclin synthesis and degradation in the control of maturation promoting factor activity. Nature 339:280–286. doi: 10.1038/339280a0 PMID: 2566918

56. Minshull J, Pines J, Golsteyn R, Standart N, Mackie S, Alan C, et al. (1989) The role of cyclin synthesis, modification and destruction in the control of cell division. J. Cell Sci. Suppl. 12:77–97. doi: 10.1242/jcs.1989.Supplement_12.8 PMID: 2534558

57. Romond PC, Rustici M, Gonze D, Goldbeter A (1999) Alternating oscillations and chaos in a model of two coupled biochemical oscillators driving successive phases of the cell cycle. Ann. N. Y. Acad. Sci. 879:180–193. doi: 10.1111/j.1749-6632.1999.tb10419.x PMID: 10415827

58. Minshull J, Golsteyn R, Hill CS, Hunt T (1990) The A- and B-type cyclin associated cdc2 kinases in Xenopus turn on and off at different times in the cell cycle. EMBO J. 9:2865–2875. PMID: 2143983

59. Buendia B, Clarke PR, Felix MA, Karsenti E, Leiss D and Verde F. (1991) Regulation of protein kinases associated with cyclin A and cyclin B and their effect on microtubule dynamics and nucleation in Xenopus egg extracts. Cold Spring Harb. Symp. Quant. Biol. 56:523–532. doi: 10.1101/SQB.1991.056.01.059 PMID: 1840263

60. Press WH, Teukolsky SA, Vetterling WT, Flannery BP (1992) Numerical Recipe in Fortran. Cambridge University Press.